


RESEARCH

Open Access

EQSM-based multiuser MIMO downlink transmission for correlated fading channels



Francisco R. Castillo-Soria^{1*†} , Carlos A. Gutierrez^{1†}, Abel García-Barrientos^{1†}, Armando Arce-Casas^{1†} and Jorge Simón^{2†}

Abstract

This paper presents three multiuser multiple input-multiple output (MU-MIMO) downlink transmission strategies based on the extended quadrature spatial modulation (EQSM) system for mobile communication. The three MU-MIMO precoding strategies utilised are block diagonalisation (BD), dirty paper coding (DPC), and a combined BD-DPC strategy. We analyse and compare the performance of these three MU-MIMO-EQSM schemes with the conventional MU-MIMO spatial multiplexing (MU-MIMO-SMux) system in terms of bit error rate (BER) and detection complexity considering correlated and uncorrelated fading channels. Results show that the BD-MIMO-EQSM and DPC-MIMO-EQSM systems outperform by 2 – 3 dB in BER performance their conventional counterparts with the additional advantage of a detection complexity reduction of up to 62% for the analysed cases. For the uncorrelated fading channel, the BD technique has better BER performance for a spectral efficiency (SE) of 12 bits per channel use (bpcu), while the DPC technique has better BER performance for an SE of 8 bpcu. Considering the correlated channel, DPC suffers a deep BER degradation of up to 30 dB compared with BD. However, still in this scenario, both proposed MU-MIMO-EQSM systems outperform their conventional counterparts. In terms of detection complexity, DPC has a complexity reduction of 77% as compared with the BD technique. The BD-DPC-MIMO-EQSM hybrid system inherits the low detection complexity of DPC with the advantage of all users in the system having the same BER performance.

Keywords: Extended QSM, Spatial modulation, Multiuser MIMO, Correlated channels

1 Introduction

Multiple input-multiple output (MIMO) transmission technique has been recognised as a key technology for the implementation of future wireless communication systems [1]. Spatial modulation (SM) is a MIMO transmission technique where the array of transmit (Tx) antennas is considered as a spatial constellation, then, each Tx antenna represents a point in that constellation [2]. Ideally, from each Tx antenna to each receive (Rx) antenna exists a different channel that identifies this path. Therefore, by assuming that wireless channel changes slowly and the channel state information (CSI) is known, the receiver can determine which Tx antenna has been activated at any given time [3]. It has been shown that in comparison with

the conventional spatial multiplexing (SMux) techniques, such as vertical-Bell Laboratories Layered Space-Time (V-BLAST), SM provides a better bit error rate (BER) performance and a reduced detection complexity.

A further extension of SM, known as quadrature spatial modulation (QSM), is based on the expansion of the spatial constellation by using the real and imaginary parts of the quadrature amplitude modulation (QAM) symbols as independent information-bearing carriers on the spatial constellation [4] [5]. As a result, QSM has the advantage of doubling the number of bits that can be transmitted in the spatial constellation. Proposals for enhancing the performance of the SM/QSM scheme include for example; precoding [6], trellis code modulation [7], differential spatial modulation [8], antenna selection [9], combined QSM-spatial multiplexing (SMux) [10], and low complexity detection algorithms [11] among others.

*Correspondence: ruben.soria@uaslp.mx

[†]Francisco R. Castillo-Soria, Carlos A. Gutierrez, Abel García-Barrientos, Armando Arce-Casas and Jorge Simón contributed equally to this work.

¹Telecommunications Engineering Department, Autonomous University of San Luis Potosí, Av. Salvador Nava S/N, 78260 San Luis Potosí, Mexico
Full list of author information is available at the end of the article

These previous research have motivated novel investigations to study the performance of SM/QSM on multiuser MIMO (MU-MIMO) schemes. Recently in [12], a generalised spatial modulation (GSM) MU-MIMO scheme was proposed for the up-link channel, and it is shown that the MU-MIMO-GSM scheme outperforms in BER and/or spectral efficiency (SE) the MU-MIMO-SM and the conventional MU-MIMO systems. In [13], a precoding matrix is used to transmit an MU-SM signal for the downlink transmission. In this case, the total number of Tx antennas is divided into N_u blocks, which are independently modulated for each user by using only one Rx antenna per user. It is shown in this case that the utilised precoding matrix is an effective way to avoid MU interference. An MU-MIMO transmission system that uses SM to transmit additional broadcast information over the conventional MU-MIMO scheme was proposed in [14]. Results in [14] show that some broadcast transmission bits can be added to the conventional MU-MIMO-SMux scheme transmission without performance impairments at the cost of a slightly increased detection complexity. In [15] and [16], the concept of SM at the receiver side was effectively implemented in MU-MIMO systems. The potential applications of the SM/QSM-based schemes for MU-MIMO systems include the design of future networks that demand energy and spectral efficiencies, for example, Internet of Thing (IoT) applications with rate and energy efficiency improvements [17] or beyond 5G systems where the spatial dimension could be used as a second layer to transfer additional information [18] [19].

More recently, an extended QSM (EQSM) transmission system which combines K QSM constellations to boost the SE by a factor of K was proposed. The EQSM system employs the average powers of the QSM constellations as an additional modulation dimension for the transmission of information bits [20]. As a result, EQSM has improved SE and also shows BER performance improvements. However, the EQSM scheme was evaluated only for a Rayleigh channel model and the single-user case.

Motivated by the emerging concept of massive MU-MIMO systems, where spatial correlation is a common scenario, in this paper, two questions related to EQSM are addressed. First, what is the performance of the EQSM scheme in multiuser scenarios? And second, what is the performance of the EQSM transmission scheme for more realistic channels? Considering these questions, in this work, three different downlink MU-MIMO strategies are evaluated and compared for the EQSM transmission scheme. The three MU-MIMO downlink strategies evaluated are block diagonalisation (BD) [14], dirty paper coding (DPC) [21] and a hybrid BD-DPC strategy. The proposed systems are analysed and compared in terms of BER performance and detection complexity versus

their conventional counterparts considering two different scenarios and the optimal maximum likelihood (ML) detection criterion.

Results show that for all analysed cases, the proposed BD-MIMO-EQSM and DPC-MIMO-EQSM systems outperform in BER performance and detection complexity of their conventional counterparts. In general, the BD technique has better BER performance while the DPC technique has the lowest detection complexity. For the correlated fading channel, DPC suffers a deep degradation in BER performance compared with BD. However, for the specific case of an SE of 8 bits per channel use (bpcu) and the uncorrelated fading channel, the proposed DPC-MIMO-EQSM system is a better BER performance for three out of four users in the system. In terms of detection complexity, the DPC technique has the lowest detection complexity. The combined BD-DPC-MIMO-EQSM system inherits the low detection complexity of DPC with the advantage of all users in the system having the same BER performance. The main contributions of this paper are as follows:

1. The EQSM transmission scheme is proposed for three different multiuser MIMO systems.
2. The three proposed MU-MIMO-EQSM systems are evaluated with respect to their detection complexity and BER performance for correlated fading channels.

The remainder of this work is organised as follows. In Section 2, the general system model of the MU-MIMO-EQSM scheme is introduced. In Section 3, MU interference cancellation for MU-MIMO-EQSM systems is presented. Section 4 describes the utilised channel model. In Section 5, optimal ML detection is described. Results of detection complexity are offered in Section 6. In Section 7, results of BER performance are analysed and discussed. Finally, in Section 8, we conclude the work.

Notation: Uppercase boldface letters denote matrices whereas lowercase boldface letters denote vectors. The transpose, Hermitian transpose, complex conjugate, and Frobenius norm of \mathbf{A} are denoted by \mathbf{A}^T , \mathbf{A}^H , \mathbf{A}^* , and $\|\mathbf{A}\|_F$, respectively. The statistical expectation is represented by $E[\cdot]$, and $\mathbf{0}$ denotes an all-zero matrix (or vector). Finally, $\mathcal{CN}(0, \sigma^2)$ is used to represent the circularly symmetric complex Gaussian distribution with variance σ^2 .

1.1 Methods

The aim of this work is to apply and compare multiuser MIMO strategies for the recently proposed EQSM transmission scheme. First, BD and DPC multiuser strategies are implemented for the EQSM scheme, then a BD-DPC-MIMO-EQSM hybrid scheme is proposed. These three schemes are compared in BER performance using Monte Carlo simulations. The detection complexity of the used

algorithms is analysed using floating point operations. We proved the proposed systems utilising correlated and uncorrelated fading channels based on a geometrical model where multipath propagation is caused by the interaction of the transmitted signal with local scatterers randomly located around the users. In order to show the advantage of the proposed schemes, we compared the performance of the proposed systems with the conventional systems based on SMux under the same conditions.

2 System model

The system model of the proposed MU-MIMO-EQSM downlink transmission scheme is presented in Fig. 1. We consider a base station (BS) with N_t transmit antennas and K independent mobile stations (MS) or users, each one with N_r -receiving antennas. Thus, the end-to-end configuration can be considered as a $(K \cdot N_r) \times N_t$ downlink MU-MIMO transmission system.

The sequence of input bits a_k intended for the k th user is first modulated by one EQSM block. Then, the output of all EQSM blocks is fed into to the precoding stage

where all signals are combined using DPC or BD techniques in order to cancel inter-user interference. Figure 2 shows the EQSM block. The EQSM block combines two QSM signals to generate an EQSM signal intended for a particular user. In this manner, the spectral efficiency of the EQSM scheme is twice of the QSM scheme.

The system can transmit $m_{EQSM} = 2(\log_2(M) + 2 \log_2(L))$ bits in each time slot for each user, where M is the size of the M -ary quadrature amplitude modulation (QAM) constellation $\mathcal{S} = \{s_1, s_2, \dots, s_M\}$ and L is the length of the EQSM block.

The mathematical model of the MU-MIMO-EQSM scheme is defined as

$$\begin{bmatrix} \mathbf{y}_1 \\ \mathbf{y}_2 \\ \vdots \\ \mathbf{y}_K \end{bmatrix} = \begin{bmatrix} \mathbf{H}_1 & \mathbf{H}_1 & \cdots & \mathbf{H}_1 \\ \mathbf{H}_2 & \mathbf{H}_2 & \cdots & \mathbf{H}_2 \\ \vdots & \vdots & \ddots & \vdots \\ \mathbf{H}_K & \mathbf{H}_K & \cdots & \mathbf{H}_K \end{bmatrix} \begin{bmatrix} \mathbf{W}_1 \tilde{\mathbf{x}}_1 \\ \mathbf{W}_2 \tilde{\mathbf{x}}_2 \\ \vdots \\ \mathbf{W}_K \tilde{\mathbf{x}}_K \end{bmatrix} + \begin{bmatrix} \mathbf{n}_1 \\ \mathbf{n}_2 \\ \vdots \\ \mathbf{n}_K \end{bmatrix} \tag{1}$$

The received signal $\mathbf{y}_k \in \mathbb{C}^{N_r \times 1}$ by the k th user is

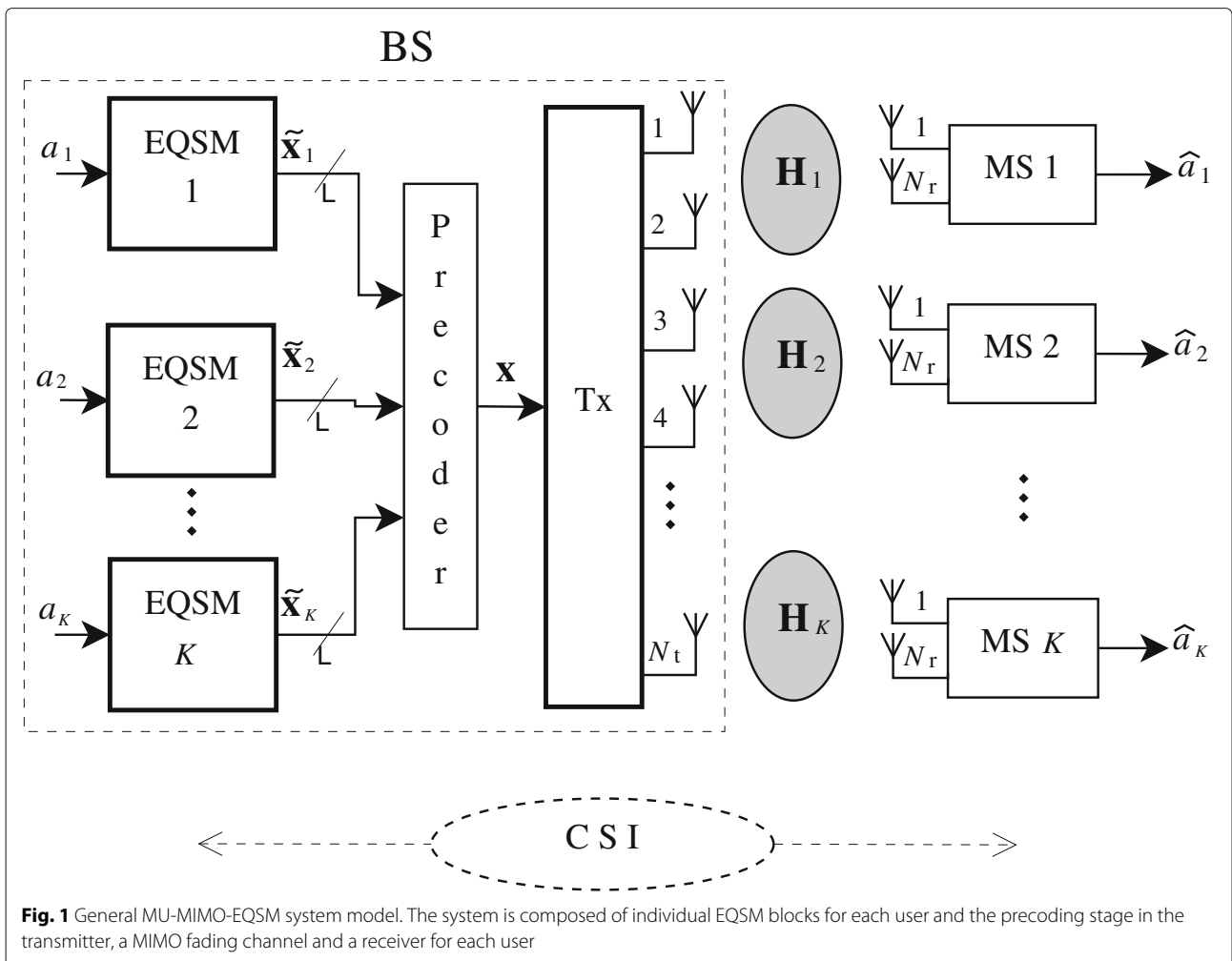


Fig. 1 General MU-MIMO-EQSM system model. The system is composed of individual EQSM blocks for each user and the precoding stage in the transmitter, a MIMO fading channel and a receiver for each user

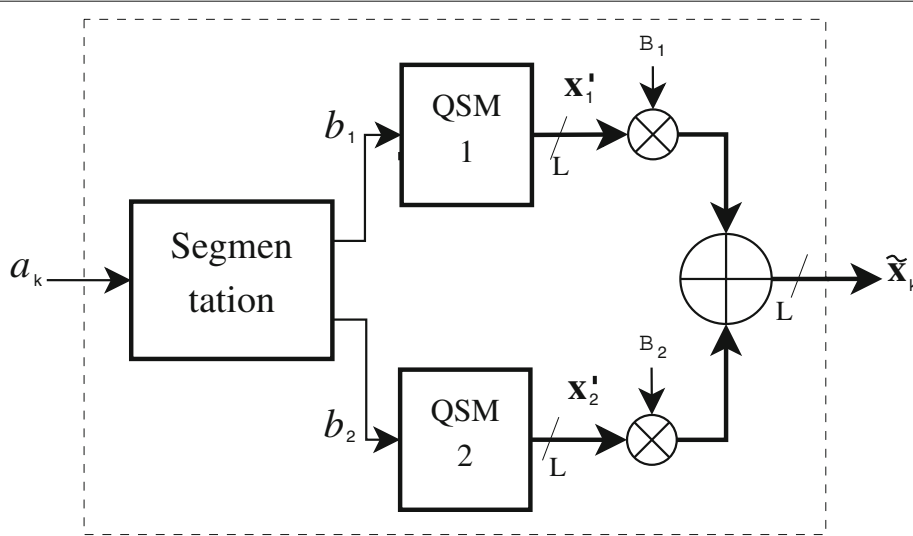


Fig. 2 EQSM transmission block. This subsystem combines the output of two QSM basic modulators

$$\mathbf{y}_k = \mathbf{H}_k \sum_{i=1}^K \mathbf{W}_i \tilde{\mathbf{x}}_i + \mathbf{n}_k, \quad (2)$$

where $\mathbf{H}_k \in \mathbb{C}^{N_r \times N_t}$ is the channel matrix between the BS and the k th user, $\mathbf{n}_k \in \mathbb{C}^{N_r \times 1}$ is the noise vector at the k th user. In this work, we use $N_t = KN_r$ which is a typical restriction for MU-MIMO systems based on BD precoding [14]. The noise samples are assumed to be independent and identically distributed (i.i.d.) with $\mathcal{CN}(0, 1)$.

Let us consider the overall transmission vector $\mathbf{x} \in \mathbb{C}^{N_t \times 1}$ defined as

$$\mathbf{x} = \sum_{i=1}^K \mathbf{W}_i \tilde{\mathbf{x}}_i. \quad (3)$$

Then, the received signal by the k th user can be represented as

$$\mathbf{y}_k = \mathbf{H}_k \mathbf{x} + \mathbf{n}_k. \quad (4)$$

2.1 EQSM transmission block

Each EQSM transmission block generates the signal intended for one particular user (mobile station) in the system. A simple two branches EQSM scheme is mainly used because of its good BER performance and SE. Each QSM branch independently modulates a bit sequence in order to have the double of the SE in the transmission system.

For the k th user, the sequence of bits $a_k = \{b_n\}_{n=1}^m$, with $b_n \in \{0, 1\}$, is fed into each EQSM block, whose output vector $\tilde{\mathbf{x}}_k \in \mathbb{C}^{L \times 1}$ is represented by

$$\tilde{\mathbf{x}}_k = [\tilde{x}_k^{(1)}, \tilde{x}_k^{(2)}, \dots, \tilde{x}_k^{(L)}]^T. \quad (5)$$

The QSM output vectors \mathbf{x}_1 and \mathbf{x}_2 are weighted by the factors $B_1 = 1$ and $B_2 = 0.5$. Then, this signals are combined to generate the EQSM output (Fig. 2). Table 1 shows the EQSM mapping rule for the first 16 values of the input bit sequence. The EQSM output signals are generated as $s = B_1 \mathbf{x}_1 + B_2 \mathbf{x}_2$.

Table 1 Example of EQSM signals generation with $L = 2$

Input bits	QSM	QSM	Output signals
a_k	\mathbf{x}_1	\mathbf{x}_2	EQSM
0000 0000	$1 + j, 0$	$1 + j, 0$	$1.5 + 1.5j, 0$
0000 0001	$1 + j, 0$	$-1 + j, 0$	$0.5 + 1.5j, 0$
0000 0010	$1 + j, 0$	$1 - j, 0$	$1.5 + 0.5j, 0$
0000 0011	$1 + j, 0$	$-1 - j, 0$	$0.5 + 0.5j, 0$
0000 0100	$1 + j, 0$	$1, j$	$1.5 + j, 0.5j$
0000 0101	$1 + j, 0$	$-1, j$	$0.5 + j, 0.5j$
0000 0110	$1 + j, 0$	$1, -j$	$1.5 + j, -0.5j$
0000 0111	$1 + j, 0$	$-1, -j$	$0.5 + j, -0.5j$
0000 1000	$1 + j, 0$	$j, 1$	$1 + 1.5j, 0.5$
0000 1001	$1 + j, 0$	$j, -1$	$1 + 1.5j, -0.5$
0000 1010	$1 + j, 0$	$-j, 1$	$1 + 0.5j, 0.5$
0000 1011	$1 + j, 0$	$-j, -1$	$1 + 0.5j, -0.5$
0000 1100	$1 + j, 0$	$0, 1 + j$	$1, 0.5 + 0.5j$
0000 1101	$1 + j, 0$	$0, -1 + j$	$1, -0.5 + 0.5j$
0000 1110	$1 + j, 0$	$0, 1 - j$	$1, 0.5 - 0.5j$
0000 1111	$1 + j, 0$	$0, -1 - j$	$1, -0.5 - 0.5j$

The first four input bits modulate the first QSM block, the other four input bits modulate the second QSM block. Table 1 only shows the first 16 EQSM signals generated

2.2 QSM technique

In order to generate the QSM signals \mathbf{x}_i , the input sequence of bits is divided into three flows. One flow is utilised to modulate a M -QAM signal and the other two flows (spatial bits) are utilised to modulate the position in the output vector as shown in Fig. 3. For an input bit sequence of length $m_{\text{QSM}} = m_{\text{EQSM}}/2$, the first $\log_2(M)$ bits modulate an M -QAM symbol. The remaining $2\log_2(L) = m_{\text{QSM}} - \log_2(M)$ bits are divided into two flows of $\log_2(L)$ spatial bits. This spatial bits modulate the position in the output vector $\mathbf{x}_i \in \mathbb{C}^{L \times 1}$ as follows: the real part of the QAM symbol is assigned to one specific position in the output vector. The remaining $L - 1$ positions are set to zero. The imaginary part of the QAM symbol can be assigned to another one or even the same position in the output vector. Finally, these two SM signals are combined to obtain the QSM output vector [4].

3 MU interference cancellation of EQSM signals

In order to avoid the multiuser interference of the EQSM signals, two different strategies of precoding are presented in this subsection. Additionally, these two basic strategies are combined to work together on the MU-MIMO interference cancellation. The two precoding strategies used are based on the CSI knowledge on the transmission side. The first strategy utilised is BD, which is based on SVD matrix decomposition. The other interference cancellation strategy used, known as DPC, is based on LQ matrix decomposition. The main difference is that in the BD technique, all users have the same BER performance

while in DPC, all users in the system have different BER performances.

3.1 Block diagonalisation

The BD technique is based on the construction of the precoding matrix $\mathbf{W}_k \in \mathbb{C}^{N_t \times N_r}$. This precoding matrix uses CSI in order to cancel all the interfering signals in the system. As shown in Fig. 4, first, the output vector $\tilde{\mathbf{x}}_k$ intended for the k th user is precoded using the matrix \mathbf{W}_k . Then, all these precoded signals are linearly combined to generate the output vector \mathbf{x} .

Rearranging terms in (2), the received signal for the k th user can be rewritten as

$$\mathbf{y}_k = \mathbf{H}_k \mathbf{W}_k \tilde{\mathbf{x}}_k + \mathbf{H}_k \sum_{i=1, i \neq k}^K \mathbf{W}_i \tilde{\mathbf{x}}_i + \mathbf{n}_k. \quad (6)$$

The first term in (6) is the signal sent to the k th user while the second term is the interference produced by the other users in the system and the third term is the noise. The interference term can be cancelled by the channel if the precoding matrix \mathbf{W}_k is designed to satisfy

$$\bar{\mathbf{H}}_k \mathbf{W}_k = \mathbf{0}, \quad k = 1, 2, \dots, K, \quad (7)$$

where the matrix $\bar{\mathbf{H}}_k$ contains all system users' matrices except that of the k th user. Thus,

$$\bar{\mathbf{H}}_k = [\mathbf{H}_1^H, \dots, \mathbf{H}_{k-1}^H, \mathbf{H}_{k+1}^H, \dots, \mathbf{H}_K^H]^H. \quad (8)$$

In this manner, the received signal in (6) is reduced to

$$\mathbf{y}_k = \mathbf{H}_k \mathbf{W}_k \tilde{\mathbf{x}}_k + \mathbf{n}_k, \quad (9)$$

which is an interference-free signal.

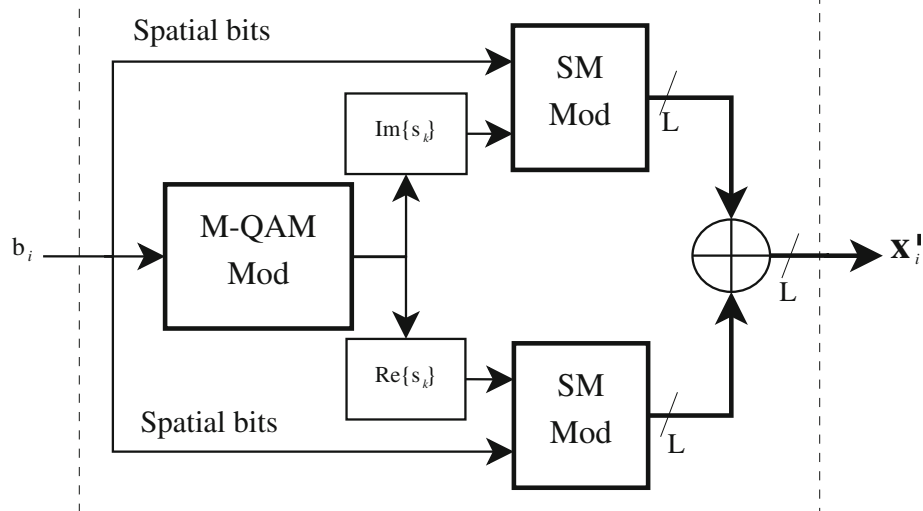
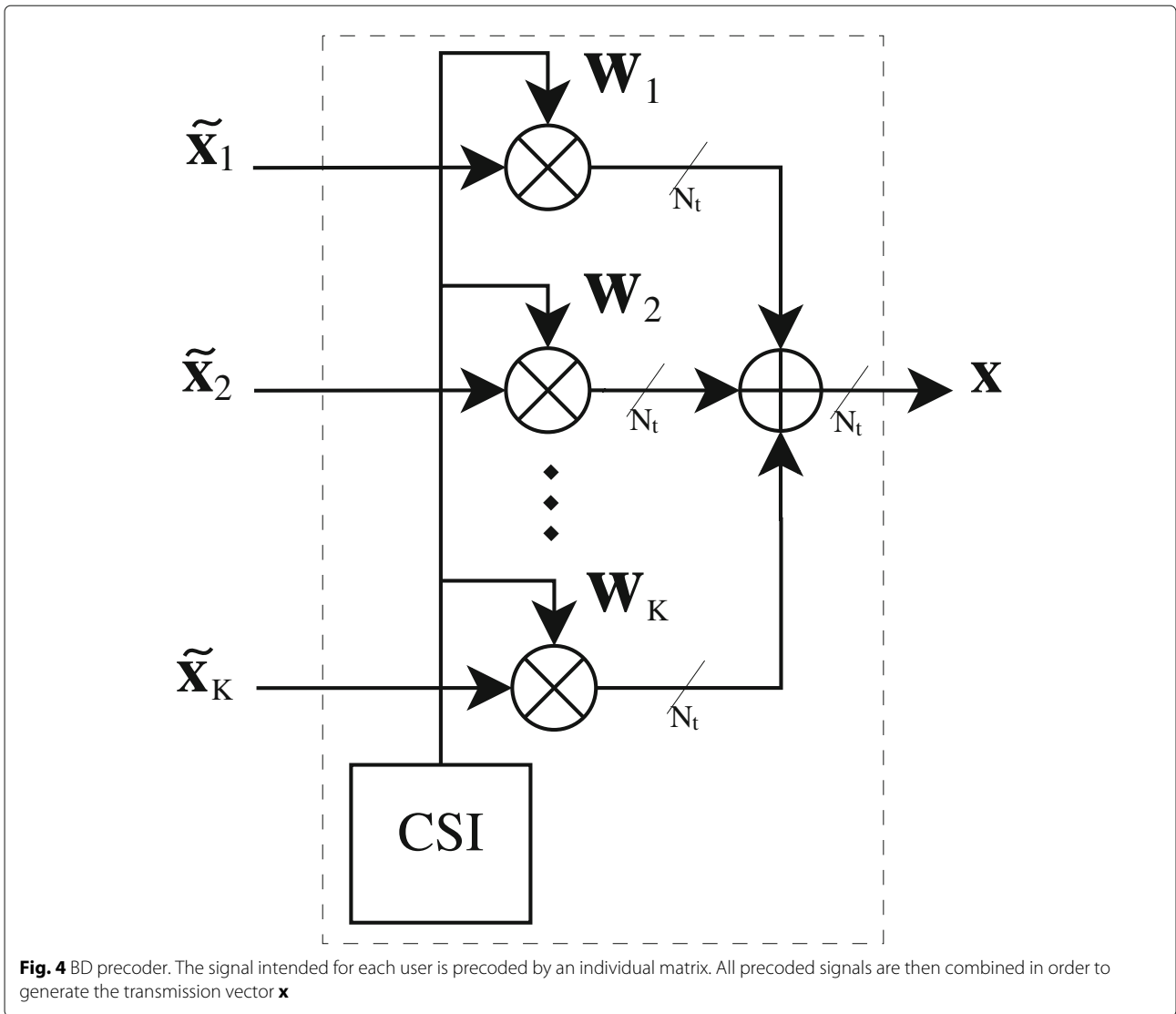


Fig. 3 QSM signal generation. The QSM subsystem combines two SM signals based on the real and the imaginary parts of the transmitted QAM symbol



The matrix \mathbf{W}_k is obtained decomposing $\bar{\mathbf{H}}_k$ into its singular values as

$$\bar{\mathbf{H}}_k = \mathbf{U}_k [\Sigma_k, \mathbf{0}] [\mathbf{V}_k^{(1)} \mathbf{V}_k^{(0)}]^H, \tag{10}$$

where \mathbf{U}_k is a unitary matrix, Σ_k is a diagonal matrix containing the non-negative singular values of $\bar{\mathbf{H}}_k$ with dimension equals to the rank of $\bar{\mathbf{H}}_k$ and $\mathbf{0}$ is an all-zero matrix. $\mathbf{V}_k^{(1)}$ contains vectors corresponding to the nonzero singular values and $\mathbf{V}_k^{(0)}$ contains vectors corresponding to the zero singular values. The matrix $\mathbf{V}_k^{(0)}$ contains the last N_r columns of \mathbf{V}_k , which form an orthogonal basis that is in the null space of $\bar{\mathbf{H}}_k$ and can be used as the precoding matrix \mathbf{W}_k .

The BD-MIMO-EQSM system can be mathematically modelled as

$$\begin{bmatrix} \mathbf{y}_1 \\ \mathbf{y}_2 \\ \vdots \\ \mathbf{y}_K \end{bmatrix} = \begin{bmatrix} \mathbf{H}_1 \mathbf{W}_1 & \mathbf{0} & \cdots & \mathbf{0} \\ \mathbf{0} & \mathbf{H}_2 \mathbf{W}_2 & \cdots & \mathbf{0} \\ \vdots & \vdots & \ddots & \vdots \\ \mathbf{0} & \mathbf{0} & \cdots & \mathbf{H}_K \mathbf{W}_K \end{bmatrix} \begin{bmatrix} \tilde{\mathbf{x}}_1 \\ \tilde{\mathbf{x}}_2 \\ \vdots \\ \tilde{\mathbf{x}}_K \end{bmatrix} + \begin{bmatrix} \mathbf{n}_1 \\ \mathbf{n}_2 \\ \vdots \\ \mathbf{n}_K \end{bmatrix} \tag{11}$$

3.2 Dirty paper coding

The DPC technique is based on the subtraction of the potential interference for each user before transmission. More specifically, the interference due to the first up to $(k - 1)$ th user signals is cancelled in the course of precoding the k th user signal [21]. As in the BD technique, DPC can be implemented when channel gains are completely

known on the transmitter. In DPC, full channel cancellation can be carried out; however, SM techniques require to have some information in the reception related to the channel, which is used for carrying extra information. Then, in the procedure proposed here, the eigenvalues of matrix \mathbf{H} are transmitted along with the QAM symbols.

First, the complete matrix channel $\mathbf{H} \in \mathbb{C}^{KN_r \times N_t}$ is \mathbf{LQ} decomposed as $\mathbf{H} = \mathbf{LQ}$. In matrix form

$$\begin{bmatrix} \mathbf{H}_1 \\ \mathbf{H}_2 \\ \vdots \\ \mathbf{H}_K \end{bmatrix} = \begin{bmatrix} l_{1,1} & 0 & \cdots & 0 \\ l_{2,1} & l_{2,2} & \cdots & 0 \\ \vdots & & \ddots & 0 \\ l_{KN_r,1} & l_{KN_r,2} & \cdots & l_{KN_r,N_t} \end{bmatrix} \begin{bmatrix} \mathbf{q}_1 \\ \mathbf{q}_2 \\ \vdots \\ \mathbf{q}_{N_t} \end{bmatrix}, \quad (12)$$

where \mathbf{L} is a lower triangular matrix and \mathbf{Q} is an unitary matrix composed by orthogonal row vectors $\mathbf{q}_k \in \mathbb{C}^{1 \times N_r}$ such as $\mathbf{Q}^H \mathbf{Q} = \mathbf{Q} \mathbf{Q}^H = \mathbf{I}$.

First, the transmission vectors $\tilde{\mathbf{x}}_k$ intended for each user are concatenated to form the vector $\tilde{\mathbf{x}} \in \mathbb{C}^{1 \times N_r}$. Then, as shown in Fig. 5, the output vector \mathbf{x} is obtained as $\mathbf{x} = \mathbf{W}\tilde{\mathbf{x}}$. The precoding matrix \mathbf{W} for the DPC technique is defined as

$$\mathbf{W} = \mathbf{Q}^H \mathbf{P}, \quad (13)$$

where the matrix \mathbf{P} is a lower triangular matrix defined as

$$\mathbf{P} = L^{-1} \begin{bmatrix} l_{1,1} & 0 & 0 \\ 0 & \ddots & 0 \\ 0 & 0 & l_{KN_r,N_t} \end{bmatrix}. \quad (14)$$

The matrix \mathbf{Q}^H cancels the orthogonal component of the channel, while the matrix \mathbf{P} is intended to deal with the inter-user interference.

Considering the transmission vector $\mathbf{x} = \mathbf{W}\tilde{\mathbf{x}} = \mathbf{Q}^H \mathbf{P}\tilde{\mathbf{x}}$. The complete array of received signals can be mathematically modelled as

$$\begin{bmatrix} \mathbf{y}_1 \\ \mathbf{y}_2 \\ \vdots \\ \mathbf{y}_K \end{bmatrix} = \begin{bmatrix} \mathbf{H}_1 \\ \mathbf{H}_2 \\ \vdots \\ \mathbf{H}_K \end{bmatrix} (\mathbf{Q}^H \mathbf{P}\tilde{\mathbf{x}}) + \begin{bmatrix} \mathbf{n}_1 \\ \mathbf{n}_2 \\ \vdots \\ \mathbf{n}_K \end{bmatrix}. \quad (15)$$

The received signal for the k th user is

$$\mathbf{y}_k = \mathbf{H}_k \mathbf{Q}^H \mathbf{P}\tilde{\mathbf{x}} + \mathbf{n}_k = \mathbf{D}_k \tilde{\mathbf{x}}_k + \mathbf{n}_k, \quad (16)$$

where $\mathbf{D}_k = \mathbf{H}_k \mathbf{Q}^H \mathbf{P}$ is a diagonal matrix. In matrix form, the received signal for the k th user is

$$\mathbf{y}_k = \begin{bmatrix} l_{1,1} & 0 & \cdots & 0 \\ 0 & l_{2,2} & \cdots & 0 \\ \vdots & \vdots & \ddots & \vdots \\ 0 & 0 & \cdots & l_{N_r,N_t} \end{bmatrix} \begin{bmatrix} x_1 \\ x_2 \\ \vdots \\ x_{N_r} \end{bmatrix} + \begin{bmatrix} n_1 \\ n_2 \\ \vdots \\ n_{N_r} \end{bmatrix}, \quad (17)$$

which is free from multiuser interference.

3.3 BD-DPC-MIMO-EQSM hybrid scheme

In this subsection, an MU-MIMO transmission system which combines BD with DPC for EQSM signals transmission is presented. It has been shown in previous works that the BD technique has good MU interference cancellation properties which result in excellent BER performance [14]. However, the main drawback of the BD technique is its high detection complexity which can be critical mainly in massive MIMO systems. On the other hand, the DPC technique has low detection complexity with relative good to medium BER performance. However, the main drawback of DPC is that all users in the system have different BER performance. Then, in order to reduce the detection complexity and at the same time obtain the same BER performance of all users in the system, a combined BD-DPC-MIMO-EQSM scheme can be implemented. In what follows, the proposed BD-DPC-MIMO-EQSM system is described.

Let us consider the signal received by the k th user using BD precoding

$$\mathbf{y}_k = \mathbf{Z}_k \tilde{\mathbf{x}}_k + \mathbf{n}_k. \quad (18)$$

where $\mathbf{Z}_k = \mathbf{H}_k \mathbf{W}_k$ is the utilised precoding.

The received signal in BD technique removes the multiuser interference. However, the inter-antenna interference produced by the MIMO channel is still present on the received signal. In order to reduce the inter-antenna interference, the transmitted signal $\tilde{\mathbf{x}}_k$ can be additionally precoded utilising a simplified version of the DPC strategy.

Utilising QR decomposition, of the matrix \mathbf{Z}_k^H , the precoded noiseless received signal by the k th user in (18) can be represented as

$$\mathbf{y}_k = \mathbf{Z}_k \mathbf{Q}(\mathbf{Z}) \mathbf{P}(\mathbf{Z}) \tilde{\mathbf{x}}_k = \text{diag}(\mathbf{R}^T) \tilde{\mathbf{x}}_k, \quad (19)$$

where $\mathbf{P}(\mathbf{Z}) = (\mathbf{R}^T)^{-1} \text{diag}(\mathbf{R}^T)$. The obtained signal is more simple and therefore has a reduced detection complexity. In Sections 6 and 7, respectively, the detection complexity and BER performance of the three MU-MIMO-EQSM systems is analysed and compared considering two different SE configurations for correlated and uncorrelated fading channels.

4 Channel model

Following the modelling approach presented in [22, 23], the channel matrix \mathbf{H}_k is characterised considering multipath propagation caused by the interaction of the transmitted signal with local scatterers randomly located around the k th MS. In addition, it is assumed that the BS and the MSs are equipped with uniform linear antenna (ULA) arrays. Under these conditions, \mathbf{H}_k can be written as

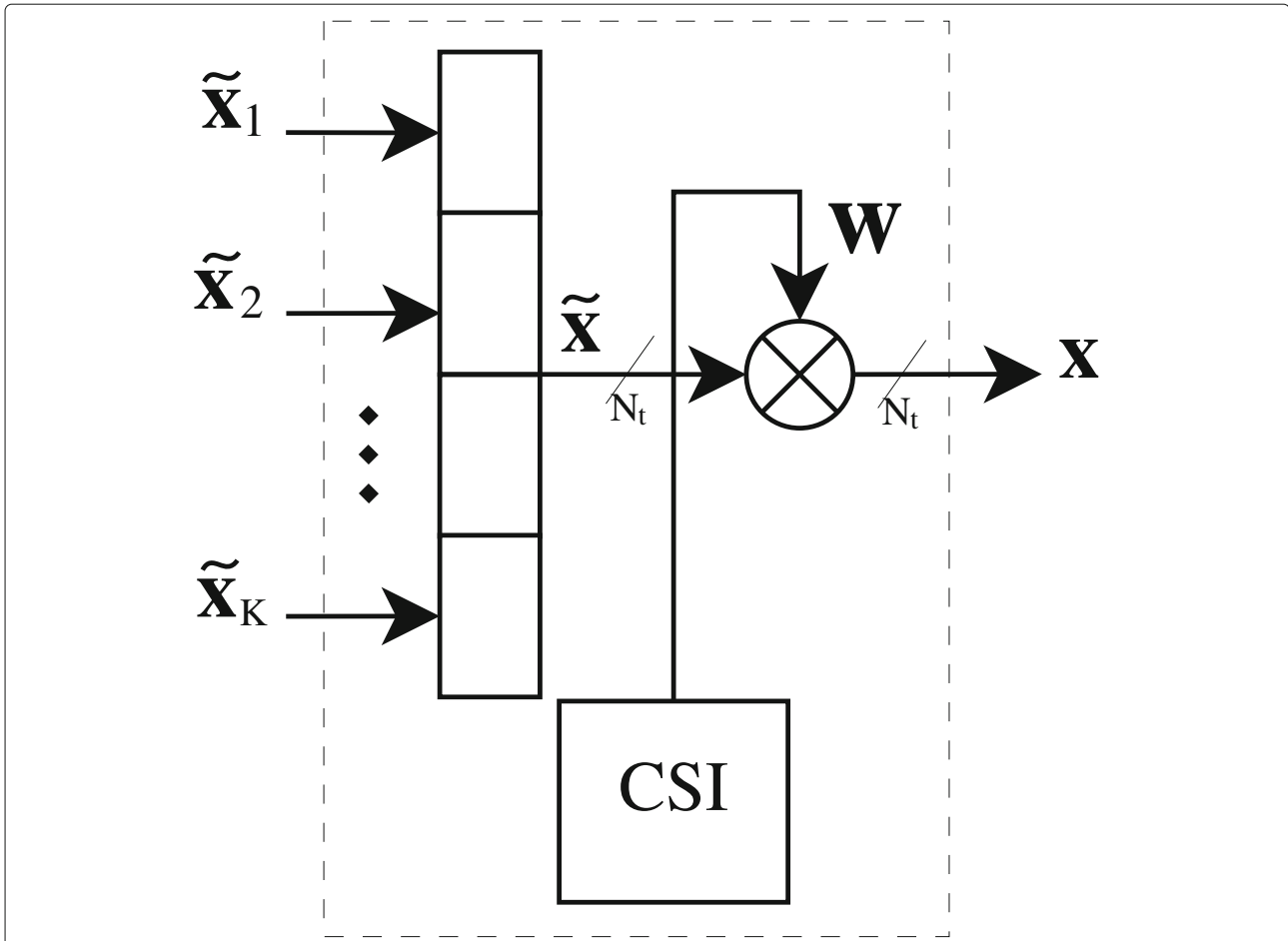


Fig. 5 DPC precoder. The signals intended for each user are first concatenated. Then, these signals are multiplied by a general precoding matrix in order to generate the transmission vector \mathbf{x}

$$\mathbf{H}_k = \sum_{\ell=1}^L g_{\ell,k} e^{-j(\theta_{\ell,k} + \psi_{\ell,k})} \mathbf{a}_r^T(\phi_{\ell}^r) \mathbf{a}_t(\phi_{\ell}^t), \quad (20)$$

for $k \in \{1, 2, \dots, K\}$. In (20), L denotes the number of local scatterers surrounding the k th MS, $g_{\ell,k}$ and $\theta_{\ell,k}$ stand for the amplitude attenuation and random phase shift, respectively, resulting from the interaction of the transmitted signal with the ℓ th local scatterer. The attenuation factors $g_{\ell,k}$ are deterministic quantities equal to $g_{\ell,k} = \sqrt{1/L}$, $\forall \ell, k$, whereas the phases $\psi_{\ell,k}$ are independent and identically distributed (i.i.d.) random variables having a uniform distribution in the interval $[-\pi, \pi]$ [23]. In turn, the phase $\psi_{k,\ell}$ is given as

$$\psi_{\ell,k} = \frac{2\pi}{\lambda} (d_{\ell,k}^t + d_{\ell,k}^r), \quad (21)$$

where $d_{\ell,k}^t$ and $d_{\ell,k}^r$ denote the distances from the BS to the ℓ th local scatterer, and from there to the k th MS, respectively, and λ stands for the carrier signal's wavelength. The

distances $d_{\ell,k}^t$ and $d_{\ell,k}^r$ can be determined based on the propagation scenario's geometrical configuration. In this paper, the distance from the k th MS to its ℓ th local scatterer is modelled by a constant quantity equal to $d_{\ell}^r = r_k$. On the other hand, the distance from the BS to the ℓ th interfering object is given as

$$d_{\ell}^t = \sqrt{D_k^2 + r_k^2 - 2r_k D_k \cos(\phi_{\ell}^r)}, \quad (22)$$

where D_k is the distance from the BS to the k th MS, and ϕ_{ℓ}^k is the angle of arrival of the ℓ th multipath component of the received signal [23]. Concerning the ULA array vectors $\mathbf{a}_r^T(\phi_{\ell}^t)$ and $\mathbf{a}_t(\phi_{\ell}^r)$, they are equal to

$$\mathbf{a}_t(\phi_{\ell}^t) = \left[e^{-jA_1^t \sin(\phi_{\ell}^t)}, \dots, e^{-jA_{N_t}^t \sin(\phi_{\ell}^t)} \right]^T, \quad (23)$$

$$\mathbf{a}_r(\phi_{\ell}^r) = \left[e^{-jA_1^r \cos(\phi_{\ell}^r)}, \dots, e^{-jA_{N_r}^r \cos(\phi_{\ell}^r)} \right]^T, \quad (24)$$

where ϕ_ℓ^t denotes the angle of departure (AOD) of the ℓ th multipath component of the received signal, and

$$A_t = \frac{\pi \Delta_t (1 - N_t)}{\lambda}, \quad A_r = \frac{\pi \Delta_r (1 - N_r)}{\lambda}. \quad (25)$$

In the previous equations, Δ_t denotes the spacing between the BS antenna elements. Likewise, Δ_r stands for the distance between the MS antenna elements. It is assumed that the angle of arrivals (AOA) ϕ_ℓ^r are i.i.d. random variables characterised by a uniform distribution on the circle. The AODs, on the other hand, are computed from the AOAs according to

$$\phi_\ell^t = \arctan \left(\frac{r_k \sin(\phi_\ell^r)}{D_k + r_k \cos(\phi_\ell^r)} \right). \quad (26)$$

In the limit when $L \rightarrow \infty$, the elements of the channel matrix defined by (20) can be modelled by complex-valued Gaussian random processes, each having a mean value equal to zero and an average power equal to one. The envelope of the resulting MIMO sub-channels is characterised by a Rayleigh distribution [24] and the spatial cross-correlation between any pair of elements of \mathbf{H}_k follows the correlation model proposed in [22].

5 Reception

In the reception, the optimal ML detection criterion is utilised in order to recover the transmitted signals. The ML criterion compares the received signal \mathbf{y}_k with all possible Tx signals in the reception in order to find the most likely one. The ML criterion for the BD-MIMO-QSM scheme is defined as

$$\hat{\mathbf{x}}_k = \arg \min_j \left\| \mathbf{y}_k - \mathbf{H}_k \mathbf{W}_k \tilde{\mathbf{x}}_k^{(j)} \right\|^2. \quad (27)$$

This formulation is simplified for the DPC-MIMO-QSM and the BD-DPC-MIMO-QSM schemes as

$$\hat{\mathbf{x}}_k = \arg \min_j \left\| \mathbf{y}_k - \mathbf{D}_k \tilde{\mathbf{x}}_k^{(j)} \right\|^2. \quad (28)$$

In Sections 6 and 7, these formulas are used in order to evaluate the detection complexity and BER performance of all analysed schemes.

6 Detection complexity

The complexity γ of the detection algorithm is measured using the total number of floating-point operations (flops) [25]. For real additions and multiplications, one flop is carried out. For complex additions and multiplications, two and six flops are carried out, respectively, while for subtractions and divisions, it will take the same value in flops as in addition and multiplication, respectively. Multiplication of $m \times n$ and $n \times p$ complex matrices uses $8 mnp$ flops [25]. Table 2 summarises all operations used for the complexity calculation of the MU-BD-ML scheme.

For the conventional BD-MIMO-SMux scheme, the lattice for the ML detector is composed as

$$\mathbf{G}_k = \mathbf{H}_k \mathbf{W}_k \mathbf{B}, \quad (29)$$

where $\mathbf{H}_k \in \mathbb{C}^{N_r \times N_t}$ and $\mathbf{W}_k \in \mathbb{C}^{N_t \times N_r}$. Multiplication of $\mathbf{H}_k \mathbf{W}_k$ requires $8N_t N_r^2$ flops and generates a square matrix of dimension $N_r \times N_r$. This matrix multiplies the matrix $\mathbf{B} \in \mathbb{C}^{N_r \times 2^m}$ and requires $8N_r^2 (2^m)$ flops. Each point in matrix \mathbf{B} is an M -QAM signal. Then, generating matrix \mathbf{G}_k requires $8N_r^2 (N_t + 2^m)$ flops. Each row in this matrix is used for a different Rx antenna.

Differences use $2(2^m)N_r$ flops. Obtaining the magnitude requires $3(2^m)N_r$ flops. Combining all results in a maximum ratio combiner (MRC) requires $2(N_r - 1)2^m$ flops and finding the minimum requires $2(2^m)$ flops. Adding all this results, the complexity of BD-MIMO-SMux scheme can be approximated as

$$\eta_{\text{BD,ML}} \approx 8N_r^2 (N_t + 2^m \beta) + 7N_r (2^m \beta) \text{ flops}. \quad (30)$$

In (30), we have introduced the factor β to consider the cases where the size of the constellation can be reduced by the inserted zeros, which is the case of EQSM. For the BD-MIMO-SMux system $\beta = 1$.

The detection complexity of the conventional DPC-MIMO-SMux system can be easily evaluated utilising the detection complexity of the BD-MIMO-SMux scheme. The main difference is that DPC avoids the multiplication of \mathbf{H}_k and \mathbf{W}_k matrices, which is substituted by only a real value derived from the diagonal matrix $\text{diag}(\mathbf{L})$. The detection lattice is conformed by the multiplication of matrix \mathbf{B} and a real number, which uses $2N_r (2^m)$ flops. As in BD-SMux, the MRC uses $7N_r (2^m)$ flops. Then, the complexity of the DPC-MIMO-SMux system can be approximated as

$$\eta_{\text{DPC,ML}} \approx 9N_r (2^m \beta) \text{ flops}. \quad (31)$$

Again, $\beta = 1$ for the conventional scheme.

The detection complexity of the BD-MIMO-EQSM and DPC-MIMO-EQSM schemes can be easily obtained using (30) and (31) and considering the number of zeros inserted in the detection lattice \mathbf{B} . The reduction factor β for EQSM can be computed as the number zeros used by the EQSM constellation divided by the total quantity of complex signals in the conventional constellation.

In the EQSM-based systems, two M -QAM symbols are transmitted at a time. However, the same Tx antenna can be used for both symbol transmissions which increases the number of zeros in \mathbf{B} . It means that the complexity of EQSM is at most the double of the QSM/SM systems complexity.

Since EQSM-based systems transmit only the real or imaginary part of a M -QAM symbol, they operate with a

Table 2 Comparison of detection complexity (γ)

Configuration/system	BD SMux	BD EQSM	PDC SMux	PDC EQSM	BD-PDC EQSM
8 bpcu	12,032	9088	4608	3456	3456
$(4 \cdot 2) \times 8$	(100%)	(76%)	(38%)	(29%)	(29%)
12 bpcu	641,024	241,664	147,456	55,296	55,296
$(4 \cdot 4) \times 16$	(100%)	(38%)	(23%)	(8.6%)	(8.6%)

The conventional BD-MIMO-SMux systems are considered as reference with 100% of complexity

complexity reduced 50%. Considering the above assumptions, the reduction factor can be approximated as

$$\beta \approx \frac{3}{2L}. \tag{32}$$

Due to the precoding technique used, the complexity of the BD-DCP-MIMO-EQSM becomes the same as the DPC-MIMO-EQSM scheme. Table 2 compares the detection complexity for all schemes. In Table 2, we consider the conventional BD-MIMO-SMux system as a reference with a 100% of detection complexity.

7 Results and discussion

In this Section, $(4 \cdot 2) \times 8$, (8 bpcu) and $(4 \cdot 4) \times 16$, (12 bpcu) configurations are utilised over correlated and uncorrelated fading channels in order to compare the BER performance of the five systems. All systems are compared considering the same SE and a normalised transmission power of $E[\mathbf{x}^H \mathbf{x}] = K$. For simulation, we target a BER of 10^{-4} .

For the uncorrelated fading channel and an SE of 8 bpcu (Fig. 6), the BD-MIMO-EQSM system has 2 dB gain compared to the conventional BD-MIMO-SMux system used

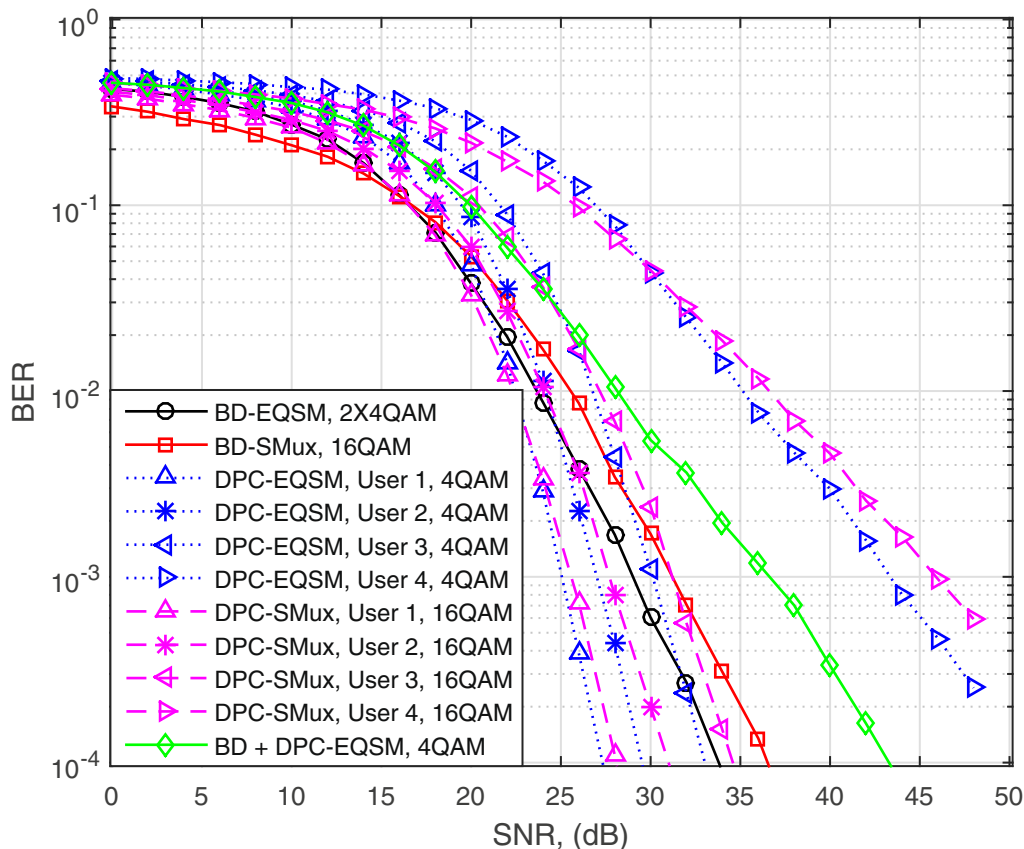


Fig. 6 BER performance comparison for an $(4 \cdot 2) \times 8$ configuration and the uncorrelated fading channel. This figure compares the three proposed MU-MIMO-EQSM schemes with the conventional ones considering an spectral efficiency of 8 bpcu for all systems

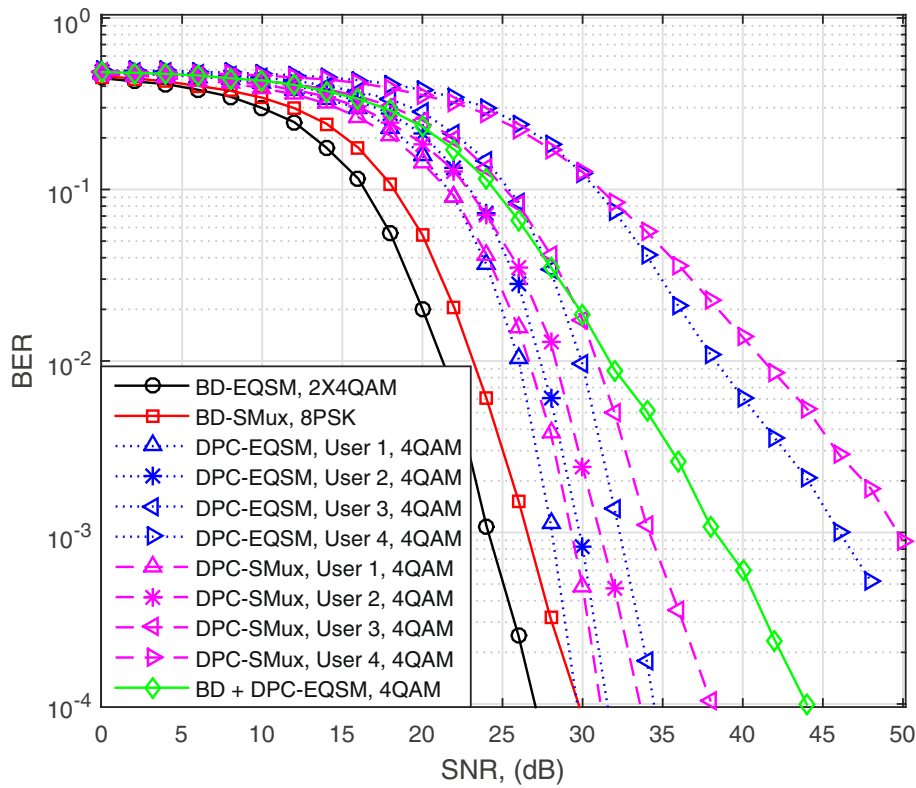


Fig. 7 BER performance comparison for an $(4 \cdot 4) \times 16$ configuration and the uncorrelated fading channel. This figure compares the three proposed MU-MIMO-EQSM schemes with the conventional ones considering a spectral efficiency of 12 bpcu for all systems

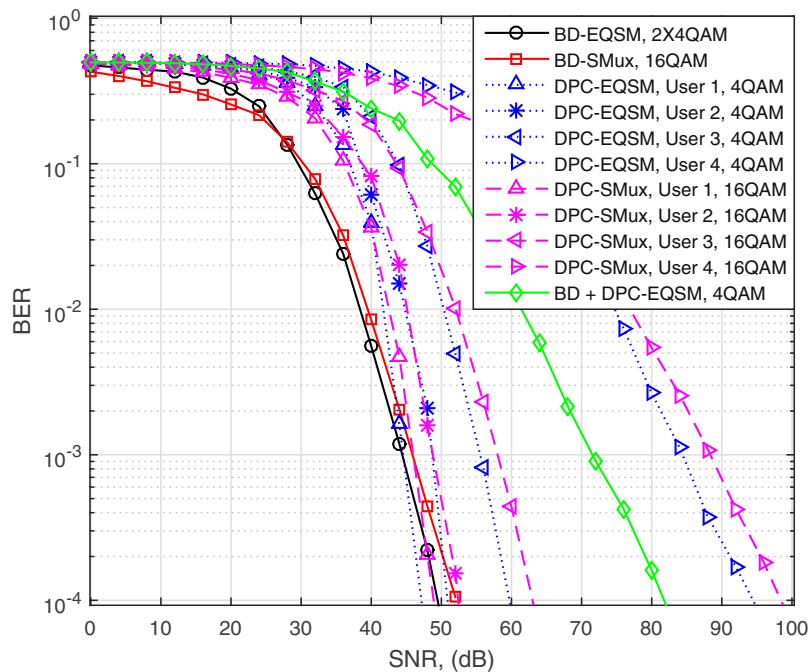


Fig. 8 BER performance comparison for an $(4 \cdot 2) \times 8$ configuration and a correlated fading channel. This figure compares the three proposed MU-MIMO-EQSM schemes with the conventional ones considering a spectral efficiency of 8 bpcu for all systems and a spatial correlated channel with Tx antennas separated by 1.5λ .

as a reference. However, the best performance is obtained by three out of four users of the DPC-MIMO-EQSM system which has gains of 6 dB, 5 dB, and 2 dB compared with the BD-MIMO-EQSM system. On the other hand, the last user in the DPC-MIMO-EQSM scheme has noticeable BER losses. Finally, the BD-DPC-MIMO-EQSM scheme has losses of 7 dB compared with the conventional BD-MIMO-SMux scheme.

For the uncorrelated fading channel and an SE of 12 bpcu (Fig. 7), the BD-MIMO-EQSM scheme has the best BER performance with 3 dB gain when compared with the conventional BD-MIMO-SMux and the best user (first user) of the DPC-MIMO-EQSM scheme. The DPC-MIMO-EQSM scheme outperforms its conventional counterpart for 2 dB approximately. Also, the BD-DPC-EQSM scheme has losses of 14 dB compared with the conventional BD-MIMO-SMux scheme.

Considering a spatial correlated fading channel with Tx antennas separated 1.5λ and SE of 8 bpcu (Fig. 8), BD-based schemes are affected in BER around 15 dB. Meanwhile, schemes using DPC are affected by 20 dB approximately. It is worth noting that the two best users of the DPC-MIMO-EQSM scheme, the BD-MIMO-EQSM, and

the conventional BD-MIMO-SMux system have approximately the same BER performance.

Considering the correlated fading channel with Tx antennas separated 1.5λ and SE of 12 bpcu (Fig. 9), the BD technique clearly outperforms the DPC technique. The correlated channel adds losses of 10 dB and 30 dB for the BD and the DPC techniques, respectively. In this scenario, the best performance is achieved by the BD-MIMO-EQSM scheme, which has 4 dB gain compared with the conventional scheme and at least 31 dB gain compared with the DPC-based multiuser schemes. Again, the BD-DPC-MIMO-EQSM hybrid system has a BER performance between the third and fourth user of the DPC-MIMO-EQSM scheme.

It is worth noting that the DPC technique is more affected by the correlated channel than the BD technique, and this is mainly because the correlation affects the singular values of the channel which are used by the DPC-based systems as the unique way to identify a particular path in the SM-based transmission. Also, the advantage of using more Tx antennas in the $(4 \cdot 4) \times 16$ configuration is severely affected when a correlated channel is used, resulting in a degradation of the BER performance.

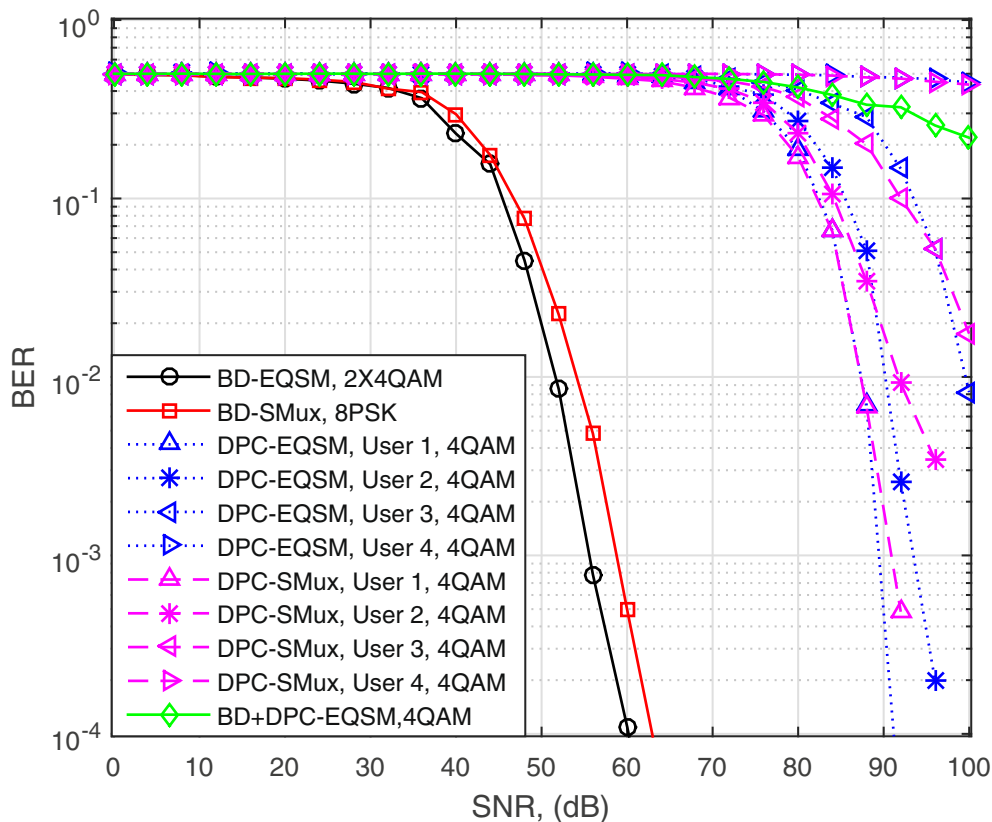


Fig. 9 BER performance comparison for an $(4 \cdot 4) \times 16$ configuration and a correlated fading channel. This figure compares the three proposed MU-MIMO-EQSM schemes with the conventional ones considering a spectral efficiency of 12 bpcu for all systems and a spatial correlated channel with Tx antennas separated by 1.5λ .

8 Conclusion

In this paper, three MU-MIMO strategies have been evaluated and compared for the recently proposed EQSM transmission scheme. The three MU-MIMO-EQSM schemes have been compared in terms of BER performance and detection complexity with their conventional counterparts for correlated and uncorrelated fading channels and optimal ML detection algorithms.

Results show that for all configurations and types of channels, the proposed BD-MIMO-EQSM and DPC-MIMO-EQSM systems outperform in BER performance and detection complexity of their conventional counterparts. More specifically, for the $(4 \cdot 2) \times 8$ configuration and considering uncorrelated fading channels, the DPC strategy outperforms the BD strategy. However, for the rest of the analysed cases, the BD-MIMO-EQSM system has the best BER performance. In particular, for the correlated fading channel, DPC schemes suffer deep degradation in BER performance, mainly for the $(4 \cdot 4) \times 16$ configuration. The hybrid BD-DPC-MIMO-EQSM scheme inherits the low detection complexity of the DPC scheme, with the advantage of all users having the same BER performance, however, suffers a deep BER performance degradation for correlated fading channels.

In conclusion, for future massive MIMO systems where a high SE is utilised and spatial correlation is typically present in the system, the proposed BD-MIMO-EQSM scheme can be the best option. In this case, low complexity detection algorithms could be implemented in order to reduce even more the detection complexity of the system.

Abbreviations

AOA: Angle of arrivals; AOD: Angle of departure; BD: Block diagonalisation; BER: Bit error rate; BS: Base station; bpcu: Bits per channel use; CSI: Channel state information; DPC: Dirty paper coding; EQSM: Extended quadrature spatial modulation; flops: Floating point operations; GSM: Generalised spatial modulation; MIMO: Multiple input-multiple output; ML: Maximum likelihood; MU: Multiuser; MS: Mobile station QAM: Quadrature amplitude modulation; Rx: Receive; SE: Spectral efficiency; SMux: Spatial multiplexing; Tx: Transmit; ULA: Uniform linear antenna

Acknowledgements

Not applicable.

Authors' contributions

FRCS and AAC conceived the main idea and analysed the results. CAG proposed the channel and AGB performed the experiments. FRCS and JS wrote the paper. All authors have read and approved the final manuscript.

Funding

Francisco R. Castillo Soria thanks the financial support obtained by the project FAI-UASLP-2019.

Availability of data and materials

Not applicable.

Competing interests

The authors declare that they have no competing interests.

Author details

¹Telecommunications Engineering Department, Autonomous University of San Luis Potosí, Av. Salvador Nava S/N, 78260 San Luis Potosí, Mexico. ²Unidad Académica de Ingeniería Eléctrica, Universidad Autónoma de Zacatecas 98000, Zacatecas, México.

Received: 8 August 2019 Revised: 4 December 2019 Accepted: 8 January 2020

Published online: 31 January 2020

References

1. C. X. Wang, F. Haider, X. Gao, X. H. You, Y. Yang, D. Yuan, H. M. Aggoune, H. Haas, S. Fletcher, E. Hepsaydir, Cellular architecture and key technologies for 5G wireless communication networks. *IEEE Commun. Mag.* **52**(2), 122–130 (2014)
2. Z. Bai, S. Peng, Q. Zhang, N. Zhang, OCC-selection-based high-efficient UWB spatial modulation system over a multipath fading channel. *IEEE Syst. J.* **13**(2), 1181–1189 (2019)
3. M. D. Renzo, H. Haas, A. Ghayeb, S. Sugiura, L. Hanzo, Spatial modulation for generalized MIMO: challenges, opportunities, and implementation. *Proc. IEEE.* **102**(1), 56–103 (2014)
4. R. Mesleh, S. S. Ikki, H. M. Aggoune, Quadrature spatial modulation. *IEEE Trans. Veh. Technol.* **64**(6), 2738–2742 (2015)
5. A. Younis, N. Abuzgaia, R. Mesleh, H. Haas, Quadrature spatial modulation for 5G outdoor millimeter-wave communications: capacity analysis. *IEEE Trans. Wirel. Commun.* **16**(5), 2882–2890 (2017)
6. J. Li, M. Wen, X. Cheng, Y. Yan, S. Song, M. H. Lee, Generalized precoding-aided quadrature spatial modulation. *IEEE Trans. Vehicular Technol.* **66**(2), 1881–1886 (2017)
7. Z. Yigit, E. Basar, R. Mesleh, Trellis coded quadrature spatial modulation. *Phys. Commun.* **29**, 147–155 (2018)
8. T. P. Nguyen, X. N. Tran, M.-T. Le, H. X. Nguyen, Differential spatial modulation for high-rate transmission systems. *EURASIP J. Wirel. Commun. Netw.* **2018**(1), 6 (2018)
9. S. Naidu, N. Pillay, H. Xu, Transmit antenna selection schemes for quadrature spatial modulation. *Wirel. Personal Commun.* **99**(1), 299–317 (2018)
10. F. R. Castillo-Soria, J. Cortez-Gonzalez, R. Ramirez-Gutierrez, F. M. Maciel-Barboza, L. Soriano-Equigua, Generalized quadrature spatial modulation scheme using antenna grouping. *ETRI J.* **39**(5), 707–717 (2017)
11. Z. Yigit, E. Basar, Low-complexity detection of quadrature spatial modulation. *Electron. Lett.* **52**(20), 1729–1731 (2016)
12. T. L. Narasimhan, P. Raviteja, A. Chockalingam, Generalized spatial modulation in large-scale multiuser MIMO systems. *IEEE Trans. Wirel. Commun.* **14**(7), 3764–3779 (2015)
13. S. Narayanan, M. J. Chaudhry, A. Stavridis, M. D. Renzo, F. Graziosi, H. Haas, in *2014 IEEE Wireless Communications and Networking Conference (WCNC)*. Multi-user spatial modulation MIMO, (Istanbul, 2014), pp. 671–676
14. F. R. Castillo-Soria, J. Sanchez-Garcia, M. Maciel-Barboza, J. Flores-Troncoso, Multiuser MIMO downlink transmission using block diagonalization and generalized spatial modulation techniques. *AEU - Int. J. of Electron. and Commun.* **70**(9), 1228–1234 (2016)
15. K. M. Humadi, A. I. Sulyman, A. Alsanie, Spatial modulation concept for massive multiuser MIMO systems. *Int. J. of Antennas and Propag.* **2014**, 1–9 (2014)
16. Y. Chen, L. Wang, Z. Zhao, M. Ma, B. Jiao, Secure multiuser MIMO downlink transmission via precoding-aided spatial modulation. *IEEE Commun. Lett.* **20**(6), 1116–1119 (2016)
17. X. Liu, X. Zhang, Rate and energy efficiency improvements for 5G-based IoT with simultaneous transfer. *IEEE Internet Things J.* **6**(4), 5971–5980 (2019)
18. X. Liu, X. Zhang, M. Jia, L. Fan, W. Lu, X. Zhai, 5G-based green broadband communication system design with simultaneous wireless information and power transfer. *Phys. Commun.* **28**, 130–137 (2018)
19. X. Liu, M. Jia, X. Zhang, W. Lu, A novel multichannel Internet of Things based on dynamic spectrum sharing in 5G communication. *IEEE Internet Things J.* **6**(4), 5962–5970 (2019)
20. F. R. Castillo-Soria, J. Cortez, C. A. Gutiérrez, M. Luna-Rivera, A. García-Barrientos, Extended quadrature spatial modulation for MIMO wireless communications. *Phys. Commun.* **32**, 88–95 (2019)
21. M. Costa, Writing on dirty paper (corresp.) *IEEE Trans. Information Theory.* **29**(3), 439–441 (1983)

22. D.-S. Shiu, G. J. Foschini, M. J. Gans, J. M. Kahn, Fading correlation and its effect on the capacity of multielement antenna systems. *IEEE Trans. Commun.* **48**(3), 502–513 (2000)
23. J. T. Gutiérrez-Mena, C. A. Gutiérrez, J. M. Luna-Rivera, D. U. Campos-Delgado, J. Vázquez, A novel geometrical model for non-stationary MIMO vehicle-to-vehicle channels. *IETE Tech. Rev.* **36**(1), 27–38 (2019)
24. C. A. Gutiérrez, J. T. Gutiérrez-Mena, J. M. Luna-Rivera, D. U. Campos-Delgado, R. Velázquez, M. Pätzold, Geometry-based statistical modeling of non-WSSUS mobile-to-mobile rayleigh fading channels. *IEEE Trans. Vehicular Technol.* **67**(1), 362–377 (2018)
25. M. H. A. Khan, K. M. Cho, M. H. Lee, J.-G. Chung, A simple block diagonal precoding for multi-user MIMO broadcast channels. *EURASIP J. Wirel. Commun. Netw.* **2014**(1), 95 (2014)

Publisher's Note

Springer Nature remains neutral with regard to jurisdictional claims in published maps and institutional affiliations.

Submit your manuscript to a SpringerOpen[®] journal and benefit from:

- Convenient online submission
- Rigorous peer review
- Open access: articles freely available online
- High visibility within the field
- Retaining the copyright to your article

Submit your next manuscript at ► [springeropen.com](https://www.springeropen.com)
